

BvP neurons exhibit a larger variety in statistics of inter-spike intervals than LIF neurons

Ryosuke HOSAKA ^{1*}, Yutaka SAKAI ², Tohru IKEGUCHI ¹, and Shuji YOSHIZAWA ³

¹ *Graduate School of Science and Engineering, Saitama University
255 Shimo-Ohkubo, Sakura-ku, Saitama 338-8570, Japan*

² *Faculty of Engineering, Tamagawa University, Tokyo 194-8610, Japan*

³ *Tamagawa University Research Institute, Tokyo 194-8610, Japan*

It was recently found that the leaky integrate-and-fire (LIF) model with the assumption of temporally uncorrelated inputs cannot account for the spiking characteristics of in vivo cortical neurons. Specifically, the inter-spike interval (ISI) distributions of some cortical neurons are known to exhibit relatively large skewness to variation, whereas the LIF model cannot realize such statistics with any combination of model parameters. In the present paper, we show that the Bonh oeffer-van del Pol (BvP) model incorporating the same assumption of uncorrelated inputs can, by contrast, exhibit large skewness values. In this case, the large values of the skewness coefficient are caused by the mixture of widely distributed ISIs and short-and-constant ISIs induced by a sub-threshold oscillation peculiar to Class II neurons, such as the BvP neuron.

KEYWORDS: LIF, BvP, interspike interval, statistical analysis, class

1. Introduction

Cortical neurons receive input spike signals from thousands of other neurons. The statistical properties of the input spike signals provide useful information regarding the activity of a neuronal ensemble, because the total input to a neuron reflects the activity of pre-synaptic neurons. However, it is generally difficult to observe the input signals for a neuron of a behaving animal. On the other hand, it is not as difficult to observe output spike sequences. Considering this fact, it is important to investigate the possibility that analysis of the statistics of an output sequence can reveal features of the input current, because the output sequence depends on the input current. In fact, the coefficient of variation (CV) and the skewness coefficient (SK) of inter-spike intervals (ISIs) generated by the leaky integrate-and-fire (LIF) model provide a good measure for detecting temporal correlations of inputs. This is because the values of CV and SK are limited to a small region in the CV-SK plane, whatever uncorrelated inputs the LIF neuron receives.^{1,2)} The existence of statistical coefficients lying outside of this small region suggests temporal correlation of the inputs. Moreover, the magnitude of the deviation from this region reflects the correlation time scale. Some cortical neurons generate spike sequences whose SK values are several times larger than CV values. For these neurons, the values

^{*}Present address: Aihara Complexity Modelling Project, ERATO, JST, 3-23-5-201 Uehara, Shibuya-ku, Tokyo 151-0064, Japan. E-mail: hosaka@aihara.jst.go.jp

of (CV,SK) lie outside of the small region, and the magnitude of the deviations correspond to input correlations on a scale of hundreds of milliseconds in the LIF model.²⁾

The relationship between input and output statistics generally depends on the spiking mechanism of the neuron. It is known that the spiking mechanisms of regularly spiking neurons can be classified into two classes, Class I and Class II, according to their bifurcation structures in response to a constant current injection.^{3,4)} Regularly spiking neurons discharge spikes regularly, at a constant interval, for a sufficiently large constant current. The type of bifurcation displayed is either a saddle-node bifurcation or a Hopf bifurcation in most models of regularly spiking neurons. Neurons exhibiting the saddle-node bifurcation are called “Class I” neurons, while those displaying the Hopf bifurcation are called “Class II” neurons. One characteristic difference between the two classes is in the spike frequency. The spike frequency of a Class I neuron increases continuously from zero as a function of the input current through the saddle-node bifurcation point. In contrast, the spike frequency of a Class II neuron jumps discontinuously from zero to some finite value at the Hopf bifurcation point.

Most models of regularly spiking neurons are based on the Hodgkin-Huxley equations.⁵⁾ The original Hodgkin-Huxley model consists of four coupled ordinary differential equations describing the ion-channel properties of squid nerve axons⁵⁾ and belongs to Class II. The Hodgkin-Huxley model with an A-type K^+ -channel belongs to Class I.⁶⁾ The Morris-Lecar model consists of three coupled differential equations incorporating only two essential ionic currents, the potassium current and the calcium current.⁷⁾ The original Morris-Lecar model belongs to Class II, but it becomes Class I with an appropriate modification.⁸⁾ Other simple models containing a few variables describe only spiking properties without details of ion-channels. The Hindmarsh-Rose model, which contains three variables, was proposed to describe a bursting mode as well as a regularly spiking mode.⁹⁾ In the regularly spiking mode, this model belongs to Class I. One of the commonly used models containing two variables is the Bonhöffer-van der Pol (BvP) model,^{10,11)} which is also well known as the FitzHugh-Nagumo model.^{12,13)} The BvP model belongs to Class II. The LIF model consists of a one-dimensional differential equation with an artificial threshold-and-reset mechanism. Although the LIF model cannot be classified according to bifurcation type in the same way as the other models because of the artificial threshold-and-resetting mechanism, we can classify the LIF model as Class I from the point of view of the behavior of the spike frequency.

In this paper, we consider the BvP model as a minimum model of Class II neurons and compare it with the LIF model, representing Class I behavior. We examine in the case of the BvP model whether certain statistical quantities (namely, CV and SK) are distributed in a small region in the CV-SK plane, as in the case of the LIF model. If these statistical quantities are distributed in a small region, we can conclude that the ISI statistics of the BvP model may be capable of detecting temporal correlations of inputs. If, however, they are distributed over a wider region, we will be led to conclude that the ISI statistics of the BvP model cannot be used for detecting temporal correlation.

It is important to examine differences between Class I and II neurons in response to a highly

fluctuating input, because it is known that a cortical neuron receives highly fluctuating inputs.^{14, 15)} Although Class I and II behaviors have been discussed for a constant input or a specific input pattern in most works^{4, 16–19)}, the behaviors are yet clarified for the highly fluctuating inputs.

Several works have reported differences between the responses to stochastic inputs of the BvP and LIF models.^{20, 21)} These works examined only up to the second-order ISI statistical quantities (namely, the mean ISI and CV). These differences are important to understand the differences between Class I and Class II mechanisms. However, although those works pointed out various differences between the relationships of ISI statistics and input properties, it does not provide a proper comparison, because it is difficult to normalize the space of input parameters in each model. For this reason, in this paper, we examine the third-order ISI statistics, and consider only the structures in the space of the output ISI statistics, sweeping input parameters over the entire region in order to avoid the normalization problem of input parameters. Thus, this study provides new systematic knowledge of differences between the neuron classes for fluctuating inputs, which has not been yet clarified by the conventional studies.

2. Models and methods

2.1 Uncorrelated inputs

A cortical neuron receives spike signals from thousands of pre-synaptic neurons. Each spike signal causes a slight change in the membrane potential. If each change is small enough relative to the spiking threshold, then the overall variation of the membrane potential can be approximated as continuous fluctuations. Uncorrelated continuous fluctuations are described by Gaussian noise in the form¹⁴⁾

$$I(t) = \mu + \sigma \xi(t), \quad (1)$$

where $\xi(t)$ is white Gaussian noise with zero mean and unit variance per unit time. Thus the parameters μ and σ control mean and fluctuation of inputs, respectively. In the simulations whose results are reported below these parameters were varied over the entire range in parameter space for which the mean firing rate takes biologically feasible values.

2.2 Neuron models

2.2.1 LIF model

The leaky integrate-and-fire (LIF) model has two essential mechanisms: temporal integration of inputs and a threshold-and-resetting. The dynamics is described by the equation

$$\begin{cases} \tau \dot{v} = -v + I(t), \\ \text{if } v > \theta, \text{ then } v = v_0 \text{ and } t_i = t, \end{cases} \quad (2)$$

where \dot{v} represents the temporal derivative of v . Using scale and shift transformations in v -space, we normalized the parameters so that $v_0 = 0$ and $\theta = 1$, without loss of generality.

2.2.2 BvP model

The Bonhöffer-van der Pol (BvP) model consists of a two-dimensional differential equation whose nullclines are cubic and linear functions. Using scale and shift transformations, we express the BvP

model as the following equations, without loss of generality:

$$\dot{v} = v - v^3/3 - w + I(t), \quad (3)$$

$$\tau\dot{w} = kv - w. \quad (4)$$

In this study, we used the same parameter values as Fitzhugh (1961), which yield qualitatively the same behavior as that of the original Hodgkin-Huxley equations.⁵⁾ The parameter values correspond to the case that $k = 1.25$ and $\tau = 11.25$ in Eqs.(3) and (4). We defined spike timings by using an internal variable s , in order to avoid double counting for accidental back steps:

$$\begin{cases} \text{if } s = 0 \text{ and } v > 1, \text{ then spike and set } s = 1, \\ \text{if } s = 1 \text{ and } v < 0, \text{ then set } s = 0. \end{cases} \quad (5)$$

$$(6)$$

2.3 ISI statistics

As dimensionless statistical coefficients of ISI, we introduce the second- and third-order statistical coefficients, CV and SK, defined as

$$CV = \frac{\sqrt{\overline{(T - \bar{T})^2}}}{\bar{T}}, \quad (7)$$

$$SK = \frac{\overline{(T - \bar{T})^3}}{\sqrt{\overline{(T - \bar{T})^2}}^3}, \quad (8)$$

$$\bar{T} \equiv \lim_{n \rightarrow \infty} \frac{1}{n} \sum_{i=1}^n T_i, \quad (9)$$

where T_i is the i -th ISI, determined by the series of spike timings $\{\dots, t_i, t_{i+1}, \dots\}$ as $T_i \equiv t_{i+1} - t_i$. The coefficient CV is a dimensionless measure of the interval variation, and the coefficient SK is a dimensionless measure of the asymmetry in the interval distribution. Spike event series generated by a Poisson process always gives $(CV, SK) = (1, 2)$, regardless of the firing rate.

In the following, we directly compare the coefficients CV and SK for the LIF and BvP models. This can be done because these are dimensionless quantities. By contrast, we cannot compare the mean ISI or \bar{T} directly between the models because \bar{T} is not dimensionless. However, the ratio of \bar{T} to the temporal scale of the dynamics can be compared directly between the different models. In the LIF model, the time constant corresponding to the decay to the fixed point, τ , is equal to the temporal scale of the dynamics. The time constant for the BvP model, contrastingly, depends on the state in the state space because of the nonlinearity of this model. However, with the parameter values used in this paper, the time constant of w , τ , is an upper limit on the slower time scale. Therefore, we regard τ as the time scale of the BvP model. Hence, we compare the values of (CV, SK) between the models using a fixed \bar{T}/τ .

Shinomoto et al.(1999) obtained analytical solutions for $(\bar{T}/\tau, CV, SK)$ of the LIF model with uncorrelated inputs based on established methods.^{22,23)} For the BvP model, however, it is not easy to obtain analytical solutions, and therefore we estimated $(\bar{T}/\tau, CV, SK)$ from a finite ISI sequence consisting of 10,000 ISIs obtained by numerical simulation.

3. Structure in ISI statistics space

We calculated the statistical quantities $(\bar{T}/\tau, CV, SK)$ as functions of the input parameters (μ, σ) . These input parameters were swept, and the corresponding set of values $(\bar{T}/\tau, CV, SK)$ were obtained. These values are plotted in the CV-SK plane as contour plots of \bar{T}/τ in Fig.1. Figures 1(a) and 1(b) display the structure of the ISI statistics in the CV-SK planes for the LIF model and the the BvP model, respectively. The limiting forms of the contour lines for the LIF model are described by simple arithmetical functions:

$$\begin{aligned} \bar{T}/\tau = 0 & : \\ SK & = 3CV, \end{aligned} \quad (10)$$

$$\begin{aligned} \bar{T}/\tau = \infty & : \\ SK & = \begin{cases} 2 & (CV < 1), \\ \frac{3}{2}CV + \frac{1}{2}CV^{-3} & (CV \geq 1). \end{cases} \end{aligned} \quad (11)$$

For comparison, these contour lines for the LIF model are plotted in the background as thin dotted lines.

For most spiking data of cortical neurons, the condition $\bar{T} > \tau$ is satisfied. Decay time constants of cortical neurons have been estimated to be less than 20 ms,^{24,25)} and mean firing rates are no more than approximately 50 Hz. The region in which the (CV, SK) values are confined for $\bar{T} > \tau$ is small for the LIF model in response to uncorrelated inputs (the grey regions in Fig.1(a)). It is also known that temporal correlation enlarges the region to cover the upper area.²⁾ If the (CV, SK) values obtained from biological spiking data fall in the upper area of this region, then it is suggested that the recording neuron receives temporally correlated inputs if the neuron can be faithfully described by the LIF model.

In the BvP model, the corresponding (CV, SK) region is larger than that in the LIF model and spreads over most of the upper region (the grey region in Fig.1(b)). Even the contour line for which $\bar{T}/\tau > 1$ lies in the large SK region. If the decay time constant is smaller than τ , the corresponding region will spread still more.²⁶⁾ Therefore, we can conclude that the pair (CV, SK) is not a good measure to detect temporal correlation in inputs, on the assumption that the neuron can be faithfully described by the BvP model.

We can see in Fig.1(b) that the lower boundary ($\bar{T}/\tau \rightarrow \infty$) is almost identical to that in the LIF model (the dotted line in Fig.1(b) determined by Eq.(11)). It is implied that the lower boundary is determined by some common mechanisms for both the LIF and BvP models.

4. Origin of the difference in ISI statistics

We now attempt to identify the origin of the difference between the LIF model and the BvP model with regard to ISI statistics. The input parameters μ and σ were swept for both models, with all other parameters fixed. Thus, in both cases we searched two-dimensional parameter spaces. However, the

LIF model and the BvP model differ in following points: (i) the constraint on the reset potential, (ii) the existence of refractoriness, and (iii) the existence of damped oscillation after the emission of a spike. The difference in ISI statistics between the two models may originate from some of these three differences. In following three subsections, we examined the effects of the differences.

4.1 *Constraint on the reset potential*

The number of dimensions of the differential equations is different: the BvP model consists of a two-dimensional differential equation, whereas the LIF model consists of a one-dimensional differential equation. Also, while the BvP model realizes the threshold-and-resetting mechanism by the dynamics of two variables, the LIF model has an explicit threshold-and-resetting mechanism. This difference in the threshold-and-resetting mechanism leads to difference in the constraint on the reset point. In the LIF model, the reset point v_0 is independent of the mean input μ . Contrastingly, the effective reset point in the BvP model depends on the mean input μ , because the variables are reset around the fixed point in the case of zero fluctuations, i.e., $\sigma = 0$. The statistical coefficients for the LIF model under the constraint that the reset potential be equal to the mean input μ fall on a one-dimensional curve (Fig.1(c)). Thus, we see that the BvP model exhibits a still larger variety of values of the statistical quantities (CV,SK) when the two models are subject to the same constraint. Therefore, the difference in the constraint on the reset potential can not be an origin of the difference in the variety of CV and SK values.

4.2 *Existence of refractoriness*

Another difference between the models is in refractoriness. Specifically, the LIF model does not possess refractoriness, while the BvP model does. The length of the effective refractory period in the BvP model is approximately τ for any values of the inputs. The effect of refractoriness can be simulated in the LIF model by introducing an absolute refractory period. However, such an absolute refractory period R only causes CV to be scaled by a factor of $\bar{T}/(\bar{T} + R)$ and does not influence SK. Thus, because an introduction of refractoriness into the LIF model causes only a shift of the statistical quantities (CV,SK), it cannot contribute to the variety in values of (CV,SK).

4.3 *Existence of damped oscillation*

Even the BvP model also possesses mechanisms of temporal integration and threshold-and-resetting. The ISI sequence includes ISIs determined by the first passage time after a refractory period in a diffusion process. Another type of ISI can be included as a result of Class II behavior. Figure 2(a) displays the detailed time evolution of the membrane potential v after a short impulse input in the BvP model. When the constant input level μ is sufficiently small or sufficiently large, the response to a short impulse is qualitatively the same as in the LIF model. When the input level μ is slightly smaller than the bifurcation point, however, damped oscillation is observed in the sub-threshold range. In this case, there is a high probability for spiking around the peaks of the sub-threshold oscillation for stochastic inputs, and burst-like patterns are observed (Fig.2(b)), despite the fact that the neuron model is a model of a regularly spiking neuron. The mean input level μ changes the amplitude of the

sub-threshold oscillation, which leads to a change in the probability for the spiking to be locked to the sub-threshold oscillation, which, in turn, would cause variety in the statistical quantities (CV,SK), despite the reset point constraint. Note that the sub-threshold damped oscillation after self-spikes are generally observed before the Hopf bifurcation in Class II neurons.⁴⁾

The effects of the sub-threshold oscillations are observed in ISI histograms of simulations with the BvP model (Fig.3). We can see that two ISIs are mixed: variable ISIs and ISIs determined by the sub-threshold oscillations. Various combinations of CV and SK values are produced by the various combination of the mean ISI and the fraction of two types of ISIs. For the input parameters corresponding to large value of SK (Fig.3(c)) or CV (Fig.3(f)), The ISIs by the sub-threshold oscillations are dominant, and instead, the variable ISIs follow a long-tail distribution (sub-plots in Figs.3(c) and (f)). It is considered that the key difference between the cases of large SK (Fig.3(c)) and CV (Fig.3(f)) values is the ratio of the mean ISI ($\bar{T} = 5\tau$ and 20τ) to the period of the sub-threshold oscillation.

To confirm these consideration in the entire parameter region, we examined a simple mixture of two types of ISIs. We can see in Fig.3 that spikes occurring at the first peak of the sub-threshold oscillation are dominant. Hence, the effect of ISIs determined by the sub-threshold oscillations are approximated by the effect of constant ISIs. We now try to consider a simple mixture of variable ISIs and constant ISIs. Although there are possible ways for describing this ISI mixture, one of the plausible choices is to introduce a Markov switching mechanism. Namely, ISIs were produced randomly through a current mode switching in a Markov process between the variable ISI mode and the constant ISI mode (see Fig. 4). In the variable ISI mode, every ISI was produced randomly through sampling of an ISI distribution $F_0(T)$ derived from the constrained LIF model (Fig.1(c)) with an absolute refractory period R . In the constant ISI mode, every ISI was equal to the constant value r : spikes occurred regularly at a constant interval r . The next mode was chosen independently with a probability p for the constant ISI mode and $1 - p$ for the variable ISI mode.

Markovness in switching is irrelevant to the CV and SK values, because these statistics are independent of the order of ISIs. The essential parameter is the fraction of the two types of ISIs. However, if the two types of ISIs in the BvP model switch by uncorrelated fluctuation, then the Markov switching mechanism could statistically reproduce ISI sequences produced by the BvP model. Thus, we introduced the Markov switching mechanism in the mixture of variable ISIs and constant ISIs.

The mixture of variable ISIs and constant ISIs $F_p(T)$ is expressed in terms $F_0(T)$ and p as follows;

$$F_p(T) = p \delta(T - r) + (1 - p) F_0(T), \quad (12)$$

where δ is the Dirac delta function, and T is an ISI. The statistical quantities (\bar{T} , CV, SK) of the model are easily derived from (\bar{T}_0, CV_0, SK_0) for the ISI distribution $F_0(T)$. Changing the input parameter values (μ, σ) corresponds to changing $F_0(T)$ and p in this model.

Here we set the constant ISI and the refractory period to $r = 2.5\tau$, $R = \tau$. These values are consistent with the behavior of the BvP model. Figure 1(d) plots \bar{T}/τ contour lines in the CV-SK plane obtained by sweeping $F_0(T)$ and p . We find in comparison with Figs.1(b) and Fig.1(d) that the

mixture of the variable ISI and constant ISIs yields a variety of values in the CV-SK plane, similar to that obtained with the BvP model.

The mixed ISI distribution gives a relatively large value of SK for a CV value in the case that the mixture is biased to the constant ISIs (i.e., p is large) and the mean ISI is small ($\bar{T} < 5\tau$). Such values of CV and SK are not produced by the LIF model. Contrastingly, in the case that the mean ISI is sufficiently large ($\bar{T} > 10\tau$), a large value of p leads to a large value of CV relative to the value of SK. Such values of CV and SK are obtained with the LIF model. Therefore, it is found that burst-like spike patterns do not always lead to large values of SK. To determine the values of SK, the balance of the two modes and the mean ISI are significant. The LIF model can produce burst-like spike patterns, but this balance and the mean ISI are restricted. By contrast, the BvP model can produce various types of burst-like spike patterns with various amplitudes of the sub-threshold oscillation after spiking controlled by the mean input level.

5. Discussion

In this paper, we have shown the two points that (1) a large variety in CV and SK values is observed in the BvP neuron receiving uncorrelated inputs, and that (2) such a variety is also observed in a simple mixture of variable ISIs and constant ISIs. The constant ISIs are set to be equal to the interval from a spike to the first peak of the sub-threshold damped oscillation in the BvP neuron. These two points imply a possibility that the large variety in CV and SK values of the BvP neuron may arise from the sub-threshold damped oscillation.

Class II neurons generally exhibit the sub-threshold damped oscillation after the emission of spikes.²⁷⁾ Therefore, it is also expected that a large variety in the ISI statistical quantities (CV,SK) may be observed in many Class II neurons, even in response to uncorrelated inputs. Contrastingly, state variables monotonically approach to a fixed point after a self-spike near the saddle-node bifurcation point. Therefore, the timings of firings, that is, ISIs, are determined only by the first passage time in a diffusion process. This mechanism is essentially the same as the LIF model. In addition to this similarity, the LIF model and the Class I neuron have same functions:

- A threshold is defined explicitly in both models: The threshold of the LIF model is provided artificially, but the threshold of the Class I neuron is an unstable fixed point.
- Post-spiking behavior is same in both models: In the LIF model, the time required for the membrane potential to move from reset potential to resting potential depends on the time constant of the membrane potential. In the Class I neuron, the time required to move from the reset potential, which corresponds to the point at which state variables reach at a nullcline of a variable of the membrane potential, to the resting potential depends on a time constant of a slow variable. This time constant corresponds to the time constant of the Class I neuron.
- During the oscillation, the input stimulus decides the firing frequency: In the LIF model, as the input stimulus increases, the membrane potential increases. Thus, the firing frequency is proportional to the strength of the input stimulus. In the Class I neuron, distance between the two

nullclines decides the oscillation period. The distance is proportional to the strength of the input stimulus. Although the mechanisms are different, the strength of the input stimulus decides the firing frequency in both models.

Different from the LIF model, the Class I neuron has non-zero spike width. However, the spike width does not affect the statistics of the spike trains, for the same reason of the refractoriness as we have shown in the section 4.2. Thus, the ISI statistical quantities (CV,SK) of Class I neurons are expected to be confined to a small region in the case of uncorrelated inputs. In this case, the combination of the two ISI statistical quantities CV and SK is a good measure to detect the temporal correlation of inputs.²⁸⁾ The remaining problem is to determine how in general the above conclusion can be applied to various Class I and Class II neurons.

A large variety in CV and SK values is observed in several cortical regions, e.g. the middle temporal area, the medial superior temporal area in the visual cortex, and the principal sulcus area in the prefrontal cortex.²⁹⁾ These distributions of CV and SK values are not significantly different by the regions.²⁹⁾ These facts imply existence of a mechanism common to various cortical regions. We find two possible mechanisms to reproduce such a distribution of CV and SK values: Class I neurons receiving temporally correlated inputs and Class II neurons receiving temporally uncorrelated inputs. It is known that most cortical neurons exhibit Class I excitability on standard slice preparations. This fact seems to support the former possible mechanism. However, the class of a Hodgkin-Huxley-type model can change from Class I to Class II by slight changes of the parameter values. Therefore, it is unclear whether the cortical neurons truly exhibit Class I excitability *in vivo*. Cortical neurons may switch their classes by neuromodulators. Then, it is important future issue to develop a method to determine which spiking mechanism is more plausible for observed spike data, Class I neuron receiving temporally correlated inputs or Class II neuron receiving temporally uncorrelated inputs.

Naive classification of neurons in electro-physiology is based on supra-threshold behavior in response to a constant input. According to this method of classification, both of the Class I and Class II neurons are placed in the same category, that of ‘regularly spiking neurons’. Neurons belonging to the other category, i.e., ‘bursting neurons’, are defined to produce bursting spike patterns even in response to a constant input. Class II neurons, however, exhibit burst-like spike patterns in response to a fluctuating input, while they exhibit regular spike patterns in response to a constant input. This is because the sub-threshold behavior also appears in supra-threshold behavior, due to the fluctuation of the input. Such a mixing of behavior is a common feature of threshold mechanisms. An example of such phenomena is known as ‘stochastic resonance’, in which additive noise enhances sub-threshold signals. Biological neurons are subjected to a noisy environment and greatly fluctuating inputs. For this reason, properly accounting to sub-threshold behavior is important to understand neural systems. The classification of neurons as Class I and Class II is one useful manner of thinking in order to study the effects of sub-threshold behavior.

In this study, we used a different model and compared the results obtained with it to previous

results obtained with the LIF model.²⁾ To compare Class I and Class II neurons, however, it is better to use a model that can realize both Class I and Class II behavior by adjusting its parameters. Appropriate modification of the Morris-Lecar model or the Hindmarsh-Rose model yields a model of this kind.⁸⁾ It is an important future work to analyze such models.

Acknowledgments

We thank Kazuyuki Aihara (Institute of Industrial Science, The University of Tokyo) for encouragement. This research was partially supported by Grant-in-Aid for Scientific Research on Priority Areas (Advanced Brain Science Project) (No.16015223) from MEXT to YS and Grant-in-Aid for Scientific Research (C) (Nos.13831002, 17500136) and (B) (No.163000072) from JSPS and Scientific Research on Priority Areas (Genome Information Science) (No.15014101) from MEXT to TI.

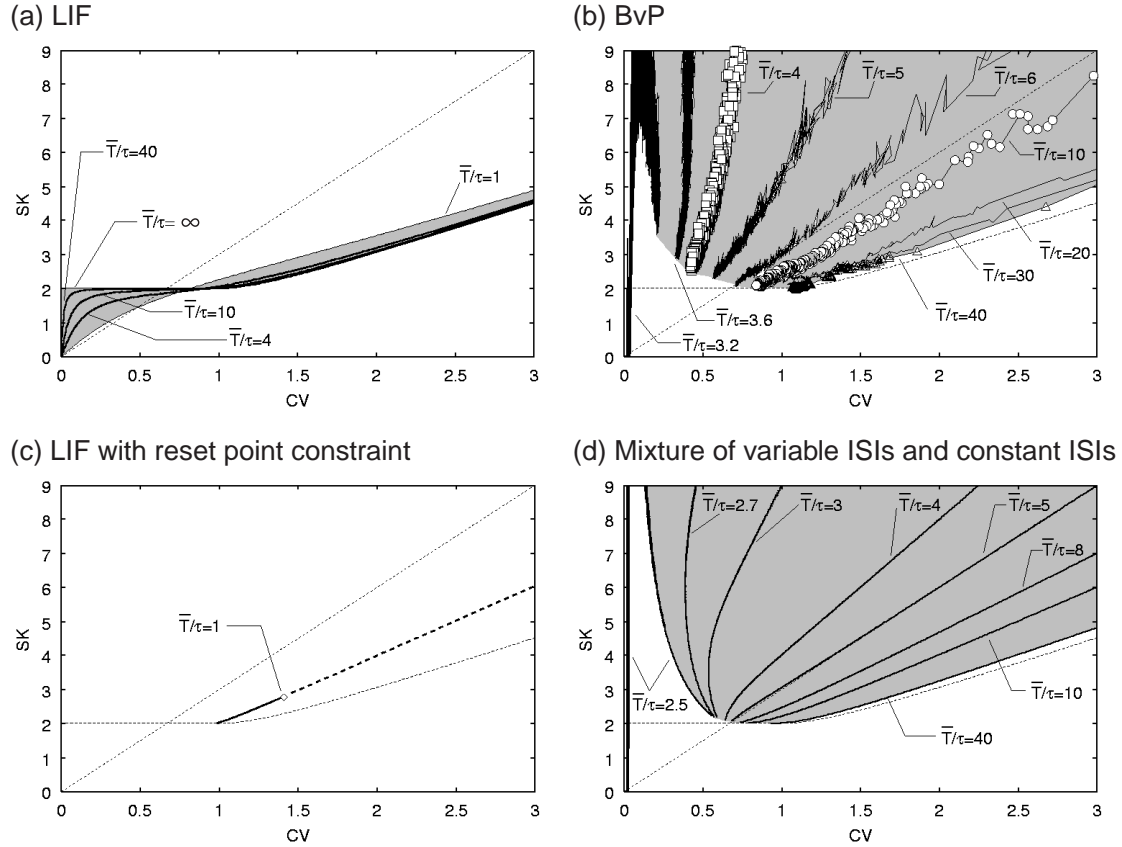


Fig. 1. Structures of the ISI statistical values $(\bar{T}/\tau, CV, SK)$ for the two models in the CV-SK plane. Contour lines of \bar{T}/τ are plotted in the CV-SK plane except in (c). The mean spike frequencies are biologically feasible (i.e., $\bar{T} > \tau$) in the grey area. The thin dotted lines appearing in all figures here are the contour lines corresponding to $\bar{T}/\tau = 0$ and $\bar{T}/\tau \rightarrow \infty$ for the LIF model. (a) Theoretical contour lines for the LIF model. (b) Contour lines for the BvP model estimated by simulation. The squares, circles and triangles correspond to data for which \bar{T} is within $\pm 1\%$ of the value satisfying $\bar{T}/\tau = 4, 10, 40$, respectively. (c) (CV,SK) (not contour lines) for the LIF model with the same constraint as in the BvP model that the reset point be equal to the fixed point, $v_0 = \mu$. (d) Contour lines for a mixture of variable ISIs and constant ISIs. The variable ISIs exhibit the ISI distribution of the LIF model with the constraint and refractory period. The constant ISI and the refractory period are set as $r = 2.5\tau$, $R = \tau$.

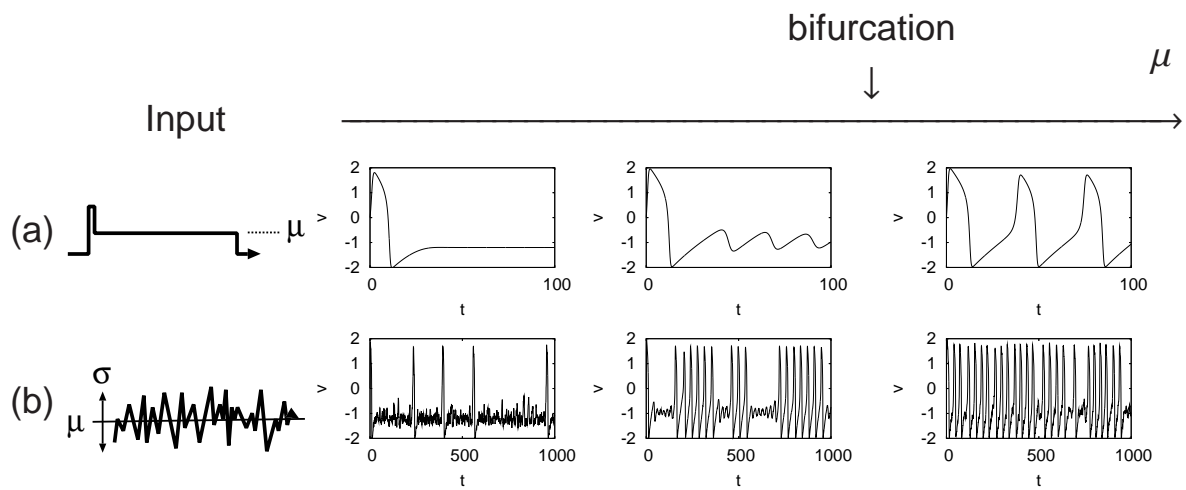


Fig. 2. Details of time evolution of v for the BvP model in response to (a) a short impulse input and (b) fluctuating inputs with various mean input levels μ . With a constant input whose level μ is slightly smaller than the bifurcation point, damped oscillation is observed in a sub-threshold range. In this case, burst-like spike patterns are observed, because there is a high probability of the spikings around the peaks of the oscillation in the case of stochastic inputs.

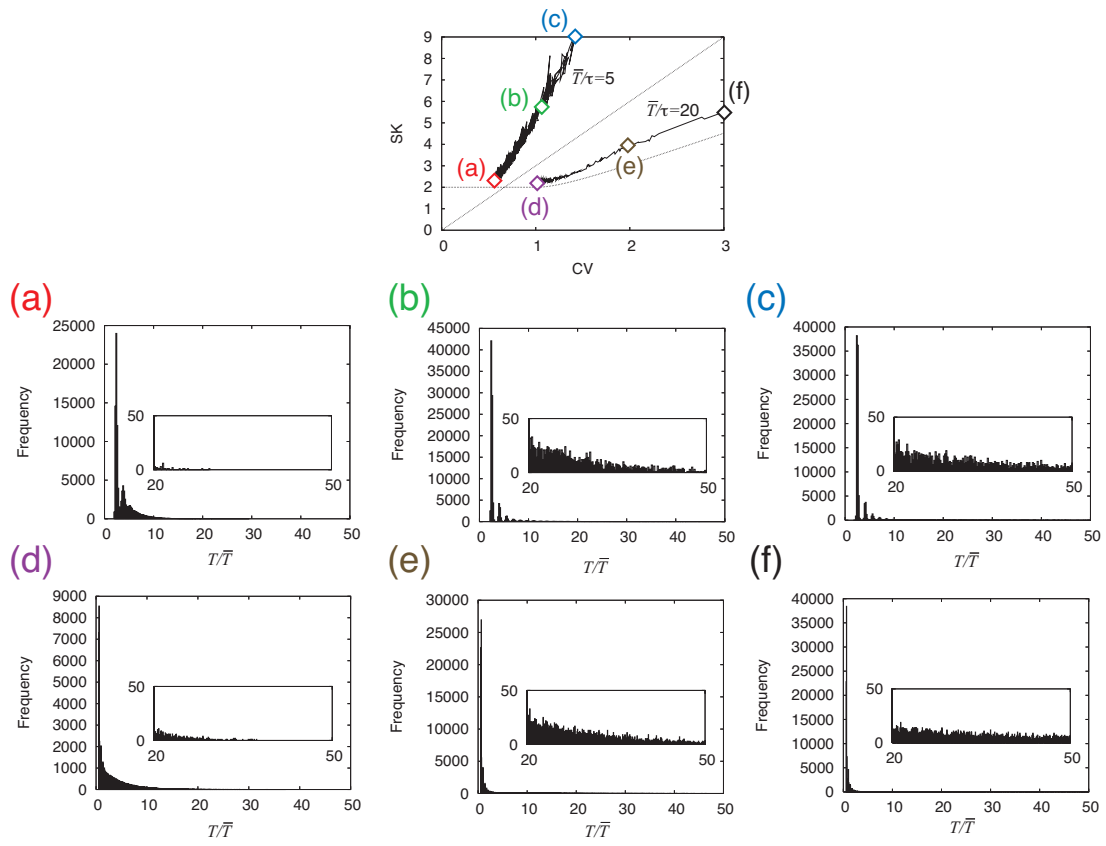


Fig. 3. The ISI histograms of the BvP model on the lines of $\bar{T}/\tau=5$ and 20. Statistical quantities of each ISI histogram correspond to the points in the upper figure.

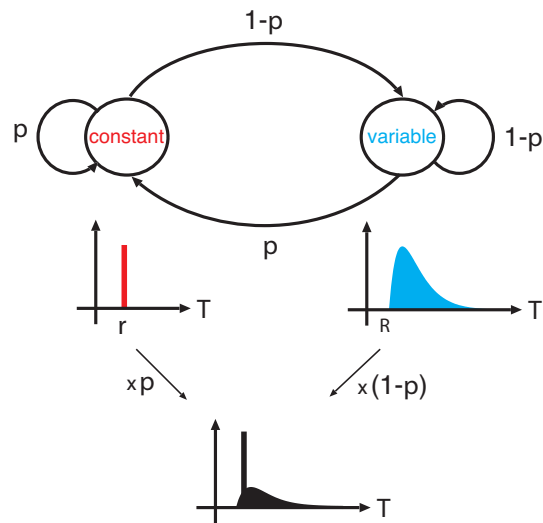


Fig. 4. Schema of the mixture of constant ISIs and variable ISIs. The ISI mixture can be produced by a Markov switching mechanism. The spiking mode switches with probability p between the constant and variable ISI modes.

References

- 1) S. Shinomoto, Y. Sakai, and S. Funahashi. The Ornstein-Uhlenbeck process does not reproduce spiking statistics of neurons in prefrontal cortex. *Neural Computation*, 11:935–951.
- 2) Y. Sakai, S. Funahashi, and S. Shinomoto. Temporally correlated inputs to leaky integrate-and-fire models can reproduce spiking statistics of cortical neurons. *Neural Networks*, 12:1181–1190.
- 3) A. L. Hodgkin. The local electric changes associated with repetitive action in a non-medulated axon. *Journal of Physiology*, 107:165–181.
- 4) E. M. Izhikevich. Neural excitability, spiking, and bursting. *International Journal of Bifurcation and Chaos*, 10:1171–1266.
- 5) A. L. Hodgkin and A. F. Huxley. A quantitative description of membrane current and its application to conduction and excitation in nerve. *Journal of Physiology*, 117:500–544.
- 6) J. A. Connor, D. Walter, and R. McKown. Neural repetitive firing modifications of the Hodgkin-Huxley axon suggested by experimental results from crustacean axons. *Biophysical Journal*, 18:81–102.
- 7) C. Morris and H. Lecar. Voltage oscillations in the barnacle giant muscle fiber. *Biophysical Journal*, 193:193–213.
- 8) J. Rinzel and B. B. Ermentrout. Analysis of neural excitability and oscillations. In C. Kock and I. Segev, editors, *Methods in Neuronal Modeling*. MIT Press, 1989.
- 9) J. L. Hindmarsh and R. M. Rose. A model of neuronal bursting using three coupled first order differential equations. *Proceeding of The Royal Society of London:Series B*, 221:87–102.
- 10) B. van der Pol. On relaxation oscillations. *Phil. Mag.*, 2:978–992.
- 11) K. F. Bonhöffer. Action of passive iron as a model for the excitation of nerve. *Journal of General Physiology*, 32:69–79.
- 12) R. Fitzhugh. Impulses and physiological states in theoretical models of nerve membrane. *Biophysical Journal*, 1:445–466.
- 13) J. Nagumo, A. Arimoto, and S. Yoshizawa. An active pulse transmission line simulating nerve axon. *Proceedings of the Institute of Radio Engineers*, 50:2061–2070.
- 14) H. C. Tuckwell. *Introduction to theoretical neurobiology*. Cambridge University Press, 1988.
- 15) M. N. Shadlen and W. T. Newsome. Noise, neural codes and cortical organization. *Current Opinion in Neurobiology*, 4:569–579.
- 16) E. M. Izhikevich. Resonate-and-fire neurons. *Neural Networks*, 14:883–894.
- 17) T. Sauer. Reconstruction of dynamical systems from interspike intervals. *Physical Review Letters*, 72:3811.
- 18) D. M. Racicot and A. Longtin. Interspike interval attractors from chaotically driven neuron models. *Physica D*, 104:184–204.
- 19) N. Masuda and K. Aihara. Filtered interspike interval encoding by class II neurons. *Physics Letters A*, 311:485–490.
- 20) D. Brown, J. Feng, and S. Feerick. Variability of firing of Hodgkin-Huxley and Fitzhugh-Nagumo neurons with stochastic synaptic input. *Physical Review Letters*, 82:4731–4734.
- 21) J. Feng and P. Zhang. Behavior of Integrate-and-Fire and Hodgkin-Huxley models with correlated inputs. *Physical Review E*, 63:051902–051913.
- 22) L. M. Ricciardi and S. Sato. First-passage-time density and moments of Ornstein-Uhlenbeck process. *Journal of Applied Probability*, 25:43–57.
- 23) J. Keilson and H. F. Ross. Passage time distribution for Gaussian Markov(Ornstein-Uhlenbeck) statistical

- process. *Selected Tables in Mathematical Statistics*, 3:233–327.
- 24) T. Kaneko, Y. Kang, and N. Mizuno. Glutaminase-positive and glutaminase-negative pyramidal cells in layer VI of the primary motor and somatosensory cortices: A combined analysis by intracellular staining and immunocytochemistry in the rat. *Journal of Neuroscience*, 15:8362–8377.
 - 25) A. M. Thomson and J. Deuchars. Synaptic interactions in neocortical local circuits: Dual intracellular recordings in vitro. *Cerebral Cortex*, 7:510–522.
 - 26) The evaluation of (CV, SK) for $\bar{T} < 3\tau$ was unstable in the present simulation, because the BvP model has an effective refractory period. Longer simulations are needed for stable computation around the refractory period.
 - 27) E. M. Izhikevich. Which model to use for cortical spiking neurons? *IEEE Trans. on Neural Networks*, 15:1063–1070.
 - 28) Experimental confirmation that (CV, SK) can be a detector of the input correlation may be realized by in vitro experiments. For example, Nowak et al, Tateno et al., and Tateno and Robinson record neural responses to fluctuated inputs.^{30–32)} If the same experiments are conducted and the coefficient SK will be estimated, the results would be a proof for our results. However, the issue is beyond the scope of this paper.
 - 29) S. Shinomoto, Y. Sakai, and H. Ohno. Recording site dependence of the neuronal spiking statistics. *Biosystem*, 67:259–263.
 - 30) L. G. Nowak, M. V. Sanchez-Vives, and D. A. McCormick. Influence of low and high frequency inputs on spike timing in visual cortical neurons. *Cerebral Cortex*, 7:487–501.
 - 31) T. Tateno, A. Harsch, and H. P. C. Robinson. Threshold firing frequency-current relationships of neurons in rat somatosensory cortex: type 1 and type 2 dynamics. *Journal of neurophysiology*, 92:2283–2294.
 - 32) T. Tateno and H. P. C. Robinson. Rate coding and spike-time variability in cortical neurons with two types of threshold dynamics. *Journal of neurophysiology*, 95:2650–2663.